# Supporting Information

# DNA Dendrimer: An Efficient Nanocarrier of Functional Nucleic Acids for Intracellular Molecular Sensing

Hong-Min Meng, Xiaobing Zhang*, Yifan Lv, Zilong Zhao, Nan-Nan Wang, Ting Fu, Huanhuan Fan, Hao Liang, Liping Qiu, Guizhi Zhu, and Weihong Tan*

Molecular Sciences and Biomedicine Laboratory, State Key Laboratory for Chemo/Biosensing and Chemometrics, College of Chemistry and Chemical Engineering, College of Biology, Collaborative Innovation Center for Chemistry and Molecular Medicine, Hunan University, Changsha 410082, China

**Corresponding Authors**

**tan@chem.ufl.edu; xbzhang@hnu.edu.cn**

## ADDITIONAL EXPERIMENTAL DETAILS

### Dynamic light scattering characterization of DNA dendrimer

The hydrodynamic diameters of the DNA dendrimer under investigation were measured using a Zetasizer Nano ZS90 DLS system equipped with a red (633 nm) laser and an Avalanche photodiode

detector (APD) (quantum efficiency > 50% at 633 nm) (Malvern Instruments Ltd., Worcestershire, England). A Kuvetten cuvette (10 mm) was used as a sample container. DLS measurements were performed at room temperature at a fixed scattering angle of 90°.

**AFM imaging**

Atomic force microscopy of samples was observed on a Multimode 8 (Bruker/USA) using ScanAsyst mode in ambient air. A 5 μL DNA sample was placed onto the surface of freshly cleaved mica and allowed to adsorb to the mica surface for approximately 30 minutes. The mica was then rinsed in Milli-Q water and dried with compressed air.

**Table S1**. Sequences of Oligonucleotides Used in This Work

| Oligonucleotide | Sequences (from 5' to 3') |
|---|---|
| $Y_{0a}$ | GAC CGA TGG ATG ACC TGT CTG CCT AAT GTG CGT CGT AAG |
| $Y_{0b}$ | GAC CGA TGG ATG ACT TAC GAC GCA CAA GGA GAT CAT GAG' |
| $Y_{0c}$ | GAC CGA TGG ATG ACT CAT GAT CTC CTT TAG GCA GAC AGG |
| $Y_{1a}$ | GAA GCC ACT CTG ACC TGT CTG ACT AAT GTG CGT CGT AAG |
| $Y_{1b}$ | GAA GCC ACT CTG ACT TAC GAC GCA CAA GGA GAT CAT GAG-BHQ1 |
| $Y_{1c\text{-}L\text{-}histidine}$ | TCA TCC ATC GGT C CAC GTG CTC GT T AAC GGG GCT |

| | |
|---|---|
| | GTG CGG CTA GGA AGT A GGA GGA G CT CAT GAT CTC CT T TAG TCA GAC AGG |
| $Y_{1c\text{-}L\text{-}histidine\text{-}R}$ | TCA TCC ATC GGT CCA CGT GCT CGT GAA GTA GCG CCG CCG TGG AGG AGC TCA TGA TCT CCT TTA GTC AGA C AG G |
| $X_{L\text{-}histidine(6)}$ | FAM-GTA AT rA GGA AGA GAT GAT GTG A |
| $X_{L\text{-}histidine(8)}$ | FAM-CTC CTC C rA GGA ACG AGC ACG TG |
| $Y_{1c\text{-}ATP（9）}$ | TCA TCC ATC GGT CCC CCC AGG TCT CAT GAT CTC CTT TAG TCA G AC AGG |
| $Y_{1c\text{-}ATP（11）}$ | TCA TCC ATC GGT CTC CCC CAG GTC TCA TGA TCT CCT TTA GTC AGA CAG G |
| $Y_{1c\text{-}ATP（12）}$ | TCA TCC ATC GGT CAC TCC CCC AGG TCT CAT GAT CTC CTT TAG TCA GAC AGG |
| $Y_{1c\text{-}ATP（13）}$ | TCA TCC ATC GGT CTA CTC CCC CAG GTC TCA TGA TCT CCT TTA GTC AGA CAG G |
| $X_{ATP}$ | FAM/Cy3-ACC TGG GGG AGT ATT GCG GAG GAA GGT |
| $X_{ATP\text{-}R}$ | FAM-ACC TGG GGG AGT AAA AAA AAA AAA AAA |
| $Y_{2a}$ | CTG TCA TCG GTC ACC TGT CTG CCT AAT GTG CGT CGT AAG |
| $Y_{2b}$ | CTG TCA TCG GTC ACT TAC GAC GCA CAA GGA GAT CAT |

| | |
|---|---|
| | GAG |
| $Y_{2c}$ | TCA GAG TGG CTT CCT CAT GAT CTC CT T TAG GCA GAC AGG’ |
| $Y_{3a}$ | GAC ACA CTG AGG TCC TGT CTG CCT AAT GTG CGT CGT AAG’ |
| $Y_{3b}$ | GAC ACA CTG AGG TCT TAC GAC GCA CAA GGA GAT CAT GAG’ |
| $Y_{3c}$ | TGA CCG ATG ACA GCT CAT GAT CTC CTT TAG GCA GAC AGG’ |
| $Y_{4a}$ | TGC TGT CTG TCC ACC TGT CTG CCT AAT GTG CGT CGT AAG’ |
| $Y_{4b}$ | TGC TGT CTG TCC ACT TAC GAC GCA CAA GGA GAT CAT GAG |
| $Y_{4c}$ | ACC TCA GTG TGT CCT CAT GAT CTC CT T TAG GCA GAC AGG |

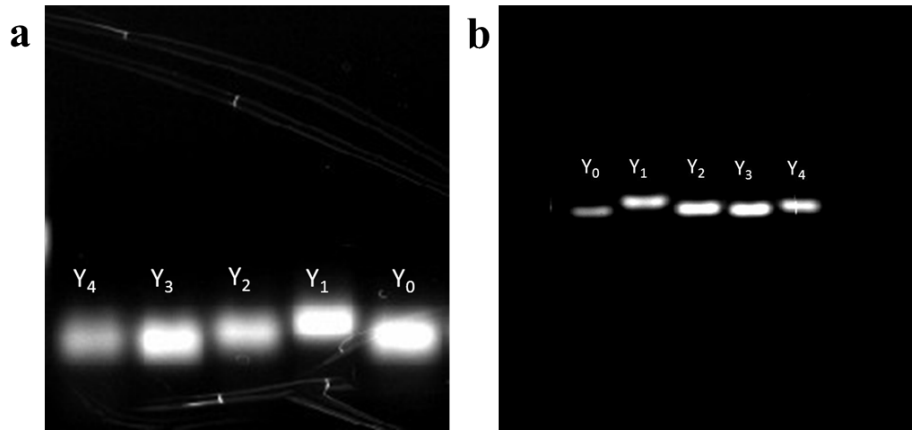


**Figure S1**. Agarose gel electrophoresis of $Y_0$–$Y_4$, (a)$Y_{\text{-L-histidine}}$, (b) $Y_{\text{-ATP}}$.

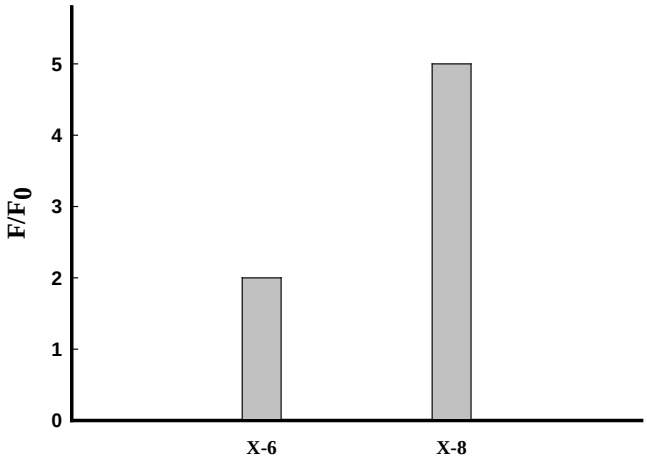


**Figure S2**.The fluorescent signal-enhanced ratio of $G_{\text{4-L-histidine}}$ with substrate strand X containing a different number of bases. The concentration of $G_{\text{4-L-histidine}}$ was fixed at 10 nM. The X-6 and X-8 denote FAM-labeled ssDNA containing 6 and 8 bases, respectively.

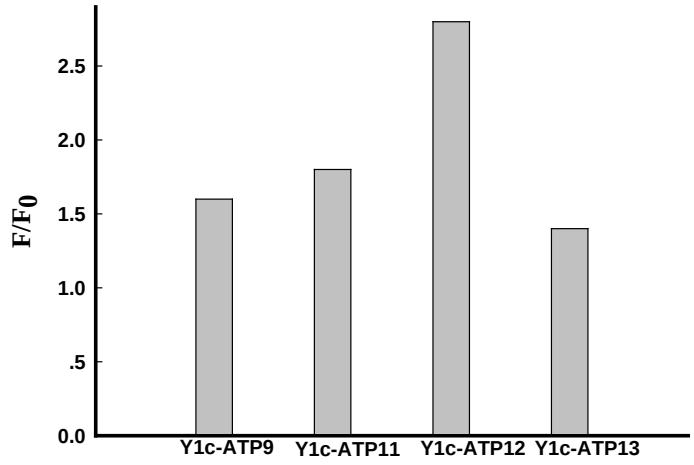


**Figure S3**. Comparison of the fluorescent signal-enhanced ratio of $G_{4\text{-ATP}}$ with $Y_{1c\text{-ATP}}$ containing a different number of bases. The concentration of $G_{4\text{-ATP}}$ was fixed at 10 nM. The $Y_{1c\text{-ATP9}}$, $Y_{1c\text{-ATP11}}$, $Y_{1c\text{-ATP12}}$, and $Y_{1c\text{-ATP13}}$ denote FAM-labeled ssDNA containing 9, 11, 12, and 13 bases, respectively.

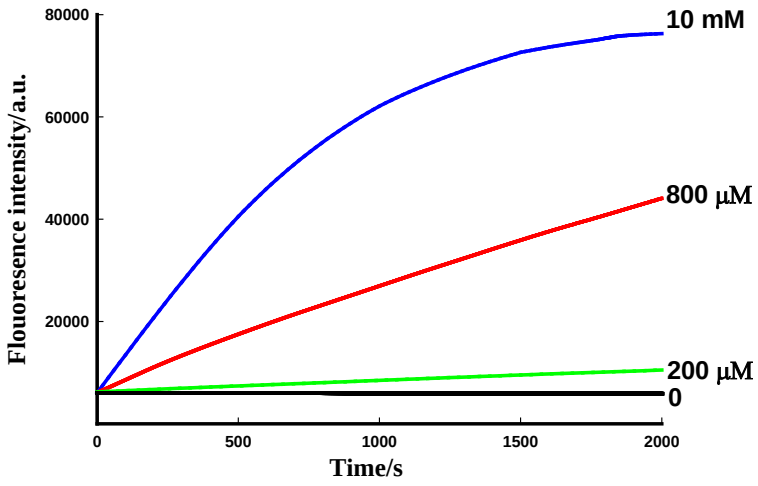


Figure S4. Time-dependent fluorescence response with low, intermediate, and high concentrations of L-histidine, the concentration for $G_{4\text{-L-histidine}}$ is 10 nM.

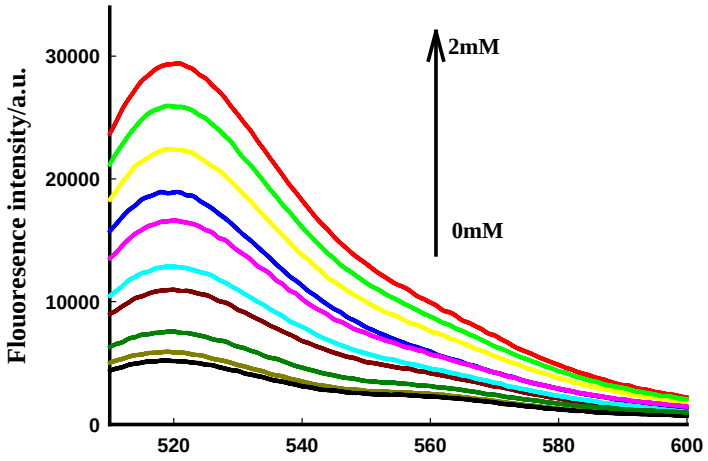


**Figure S5**. The fluorescence emission spectra of the sensing system upon the addition of ATP at different concentrations.

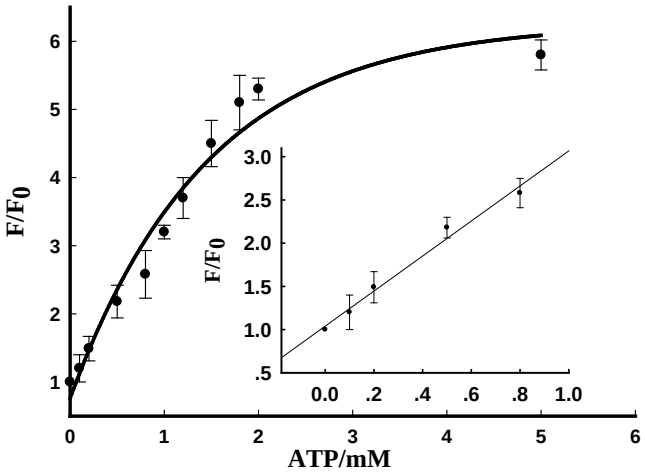


**Figure S6**.Change in fluorescence intensity based on different concentrations of ATP. Inset shows the responses of sensing system to ATP at low concentration.

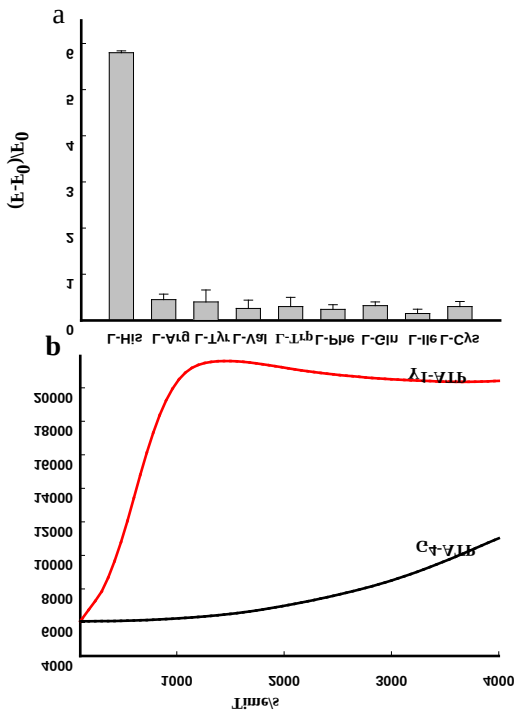


**Figure S7**. a). Selectivity of the DNAzyme-based assay for L-histidine over other potential interferences; the concentration for $G_{4\text{-L-histidine}}$ is 10 nM. b). Fluorescence kinetics spectroscopy of $G_{4\text{-ATP}}$ and $Y_{1\text{-ATP}}$ treated with 1U/mL DNase I.

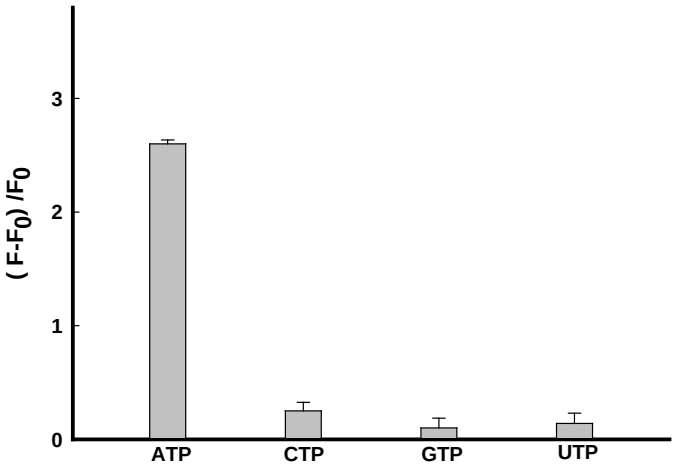


**Figure S8**. Selectivity of the aptamer-based assay for ATP compared to its analogues. The concentration for $G_{4\text{-ATP}}$ is 10 nM. $F_0$ and F are the fluorescence intensity of the sensor in the absence and presence of target, respectively.

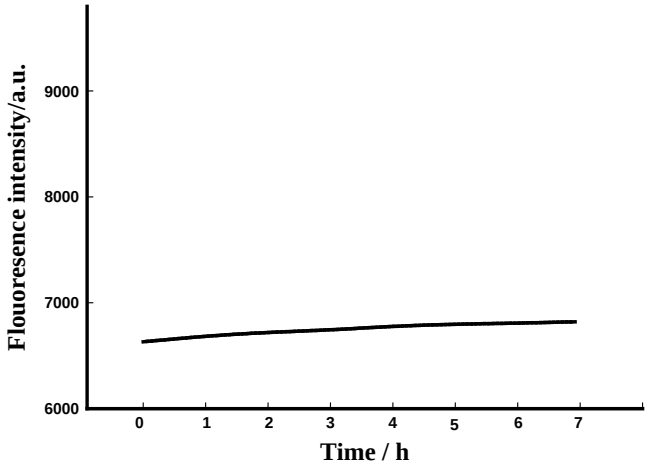


Figure S9. Fluorescence kinetics spectroscopy of $G_{4\text{-ATP}}$ treated with more than 5-hour incubation in cell lysate.

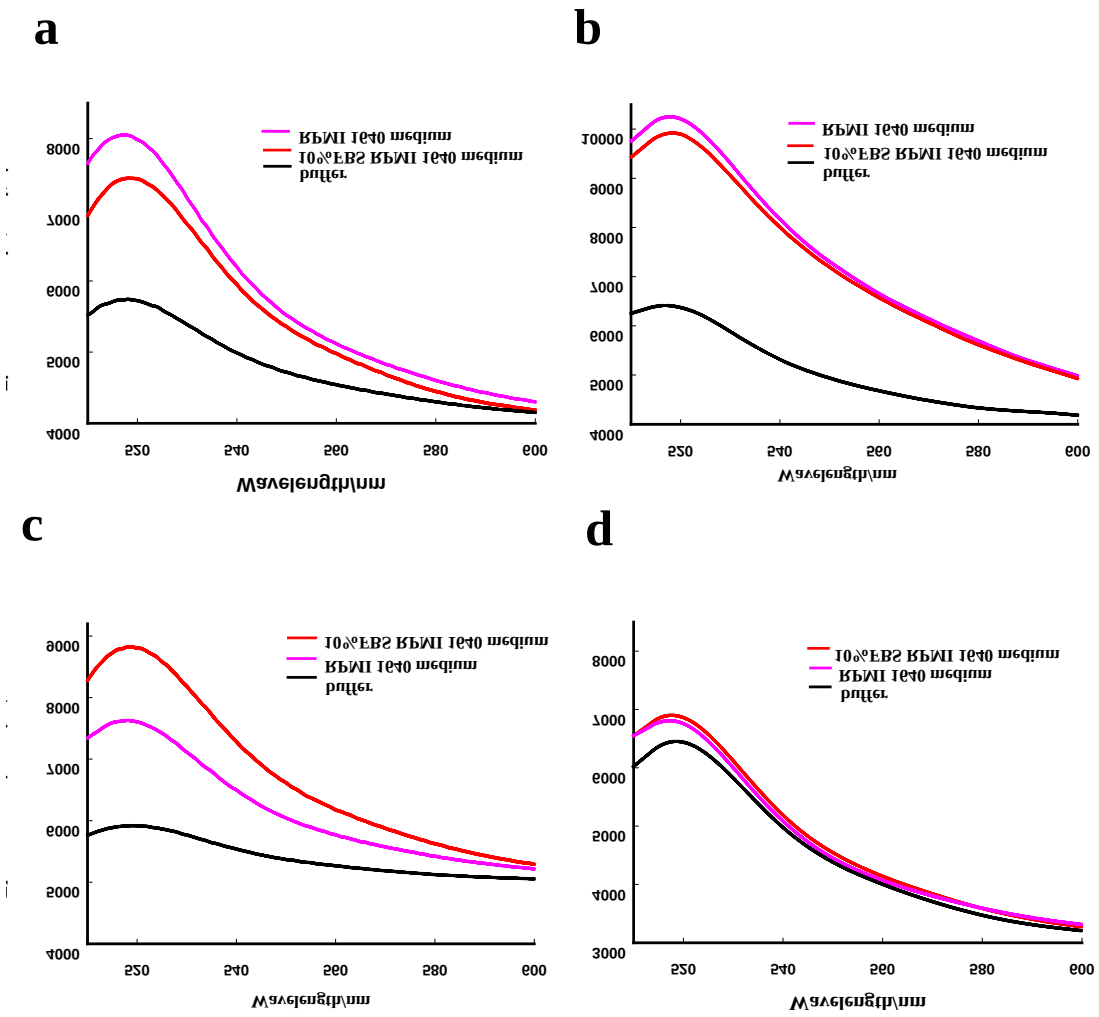


**Figure S10**. Fluorescence spectroscopy of a, $Y_{1\text{-L-histidine}}$， b, $G_{4\text{–L-histidine}}$, c, $Y_{1\text{-ATP}}$, and d, $G_{4\text{ –ATP}}$ treated with buffer, RPMI 1640 medium, and 10% FBS RPMI 1640 medium, respectively.

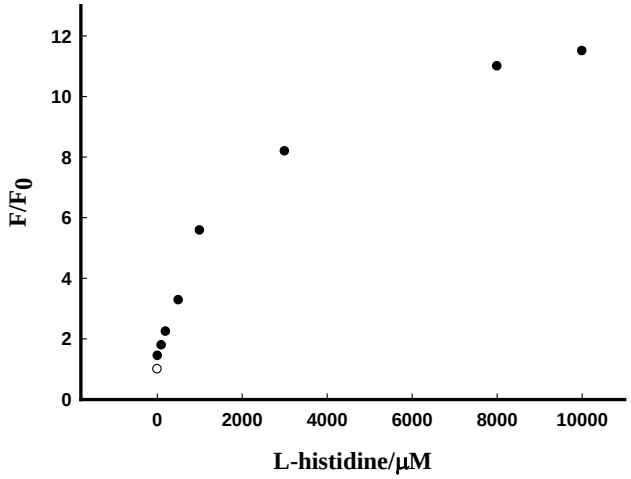


**Figure S11**. Change in fluorescence intensity based on L-histidine concentration in cell lysate samples.

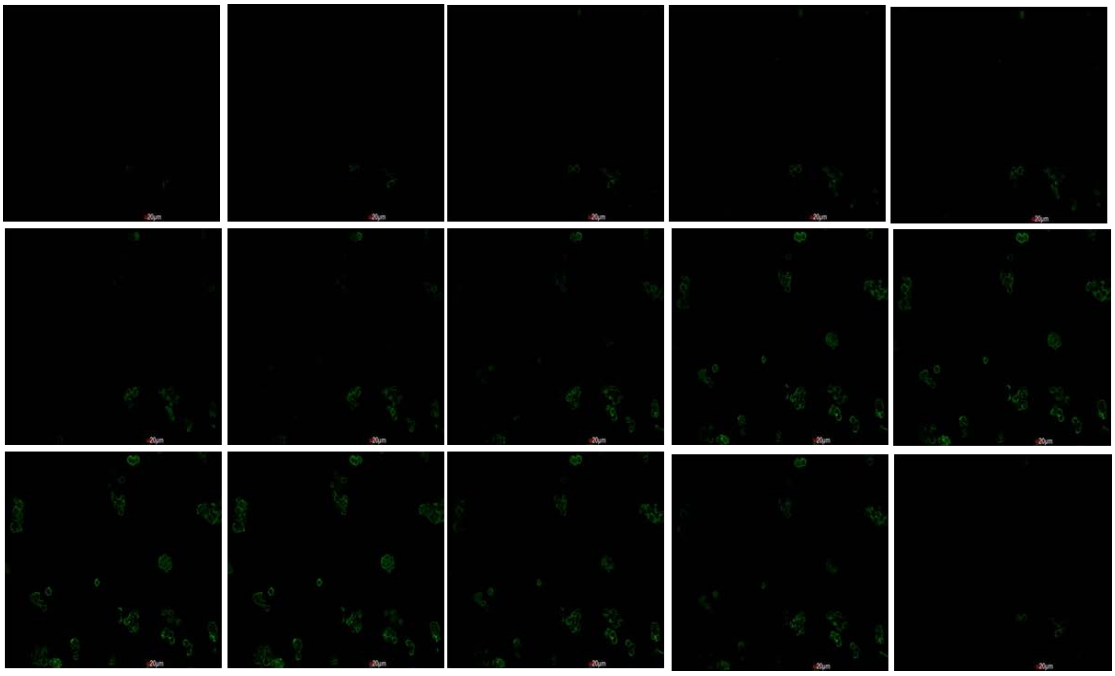

**Figure S12**. Z-stack images of cells with L-histidine, $K^+$ and active $G_{4\text{-L-histidine}}$. The green channel is FAM fluorescence from activated $G_{4\text{-L-histidine}}$, Scale bar = 20 μm.

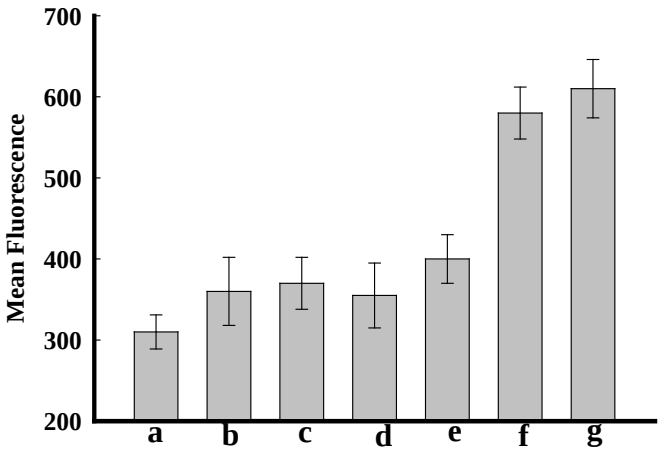


**Figure S13**. Flow cytometric quantification of cell associated fluorescence Cells a) active $G_{4\text{-L-histidine}}$. b) L-histidine and active $G_{4\text{-L-histidine}}$. c) $K^+$ and active $G_{4\text{-L-histidine}}$. d) L-histidine, $K^+$ and inactive $G_{4\text{-L-histidine-R}}$. e) random $G_{4\text{-ATP-R}}$. f) L-histidine, $K^+$ and active $G_{4\text{-L-histidine}}$. g) active $G_{4\text{-ATP}}$ were measured.

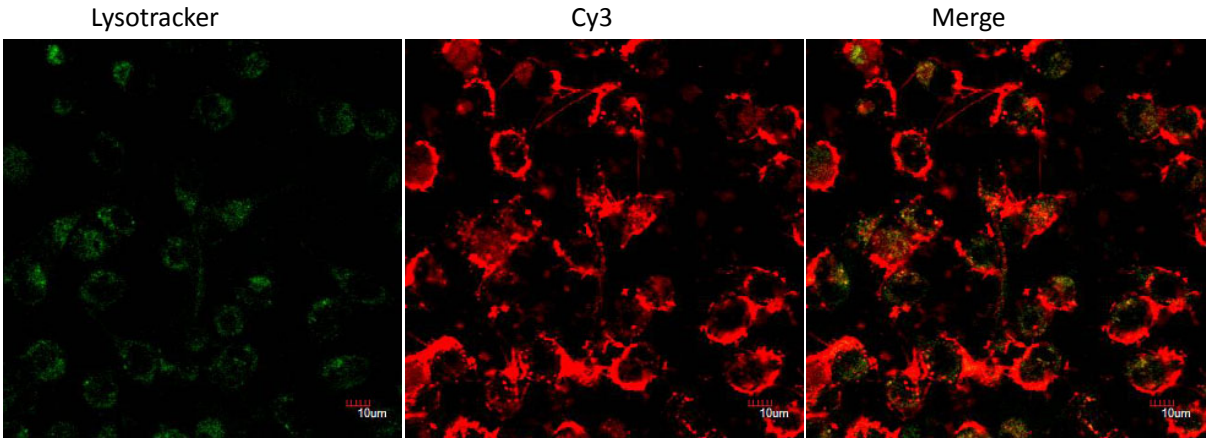


**Figure S14.** Co-localization assay of $G_{4\text{-ATP}}$ with Lysotracker. Left panels are fluorescence from Lysotracker Green staining, middle panels are Cy3 fluorescence from the $G_{4\text{-ATP}}$ probe, and right panels are the overlay of Cy3 and Lysotracker Green fluorescence. Scale bars: 10 μm.

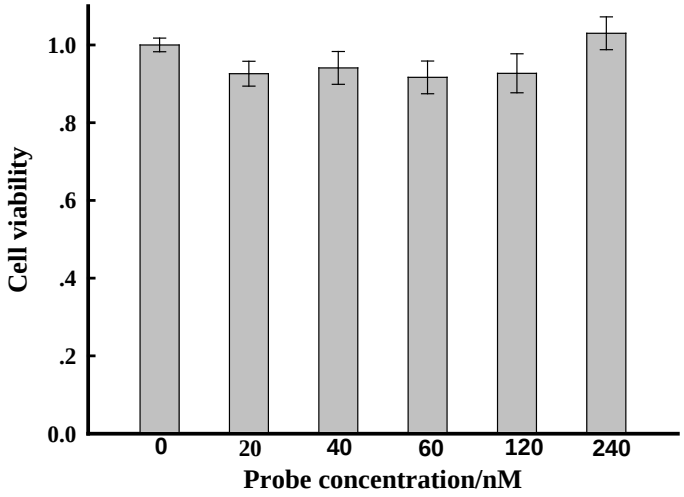


**Figure S15.** Cytotoxicity assay of MCF-7 cells treated with $G_4$ DNA dendrimers.

**References**:

(S1) Lu, L.M.; Zhang, X. B.; Kong, R. M.; Yang, B.; Tan, W. H. A Ligation-Triggered DNAzyme Cascade for Amplified Fluorescence Detection of Biological Small Molecules with Zero-Background Signal. *J. Am. Chem. Soc.* 2011, 133, 11686-11691.

(S2) Zhou, T.; Chen, P.; Niu, L.; Jin, J.; Liang, D. H.; Li, Z. B.; Yang, Z. Q.; Liu, D. S. pH-Responsive Size-Tunable Self-Assembled DNA Dendrimers. *Angew. Chem. Int. Ed.* 2012, 124, 11433-11436.